PaDIF
A Particle Detector Interaction Framework for Cosmic Rays

Bachelor thesis
to achieve the degree of
Bachelor of Science

presented by
Philipp Schlunder
born in Warburg, Germany

Lehrstuhl für Experimentelle Physik V
Fakultät Physik
Technische Universität Dortmund
2013

1. Reviewer : Prof. Dr. Dr. Wolfgang Rhode

2. Reviewer : Prof. Dr. Claus Gößling

Date of exhibition: 11. September 2013

Abstract

Within the scope of this bachelor thesis a new framework for simulations of particle-detector-interactions and based upon that two programs emulating first measurement processes are created. While the framework enables users to build various kinds of interaction settings including custom detectors, the developed programs focus on measuring cosmic particles in ice.

Contents

List of Figures

1. Introduction

In the field of astrophysics, electro-magnetic radiation is analysed in order to obtain further knowledge about the large-scaled objects of our universe. Thus, it is possible to gain information about the chemical composition and physical properties like luminosity, density or temperature by observing photon spectra of these objects. Photons are observed since they are stable, relatively easy to detect and often emitted in huge numbers while still pointing back to their source. But their spectrum extenuates due to energy dependent interactions with interstellar particles and the cosmic background radiation, complicating the information gain of energy release processes in high-energetic objects [Joh11]. This is where astroparticle physics comes into action by adding crucial information due to the analysis of other elementary particles than the photon and taking particle interaction processes into account. Possible carriers for those additional information are cosmic rays and neutrinos. Neutrinos are uncharged and weakly interacting particles. Thus, they are very unlikely to interact before reaching the earth.
However, their detection is difficult because of their low cross-section. To detect them the deposited energy, generated by charged particles created during interactions, is analysed. Those charged particles are able to emit Cherenkov radiation or bremsstrahlung which can be measured by optical detectors.
It is important to note, that neutrinos are also continuously produced by cosmic rays within particle showers in our atmosphere and on earth itself. In order to distinguish between these neutrinos and atmospheric muons a separation is necessary. That creates the need for Monte-Carlo simulations emulating particle-detector-interactions, which can be used for developing separation methods. Those methods are applied to Monte-Carlo generated data. Results are compared to the initial data set and if there is a match within an acceptable variance, these methods can be used. Furthermore measurements are smeared by the interaction with the detector, Monte-Carlo simulations are crucial again. The smearing occurs for example due to acceptance limits of sensors or influences of detector material changing a particles trajectory and draining its energy.

This thesis aims to create a simple Monte-Carlo simulation framework of particle-detector-interactions for easy data production, that can be used to develop and test new analysis methods. An in-ice detector for charged particles originating from cosmic rays and neutrinos similar to the IceCube neutrino observatory[1] is used as a proof of concept. Furthermore the framework's structure should enable a use for tutorial purposes.

[1] Information about the IceCube neutrino observatory can be found online at `http://icecube.wisc.edu/about/explained`

2. Theory

The Monte-Carlo simulation framework created within this thesis can be used to emulate an in-ice detector for charged particles deriving from cosmic rays, astrophysical or atmospheric neutrinos. In this approach IceCube, the south pole neutrino observatory, is used as a reference for two simulations. At first it is necessary to consider possible sources and interactions of both neutrinos and cosmic rays. It turns out that the index of a neutrino or cosmic ray energy spectrum is important since it contains information about the particles production processes. In order to motivate a detector simulation, the analysis chain as used in the IceCube collaboration is summarised before explaining the computational fundamentals. A description of IceCube and a detailed analysis can be found in [Mil12] and [Joh11].

2.1. Astroparticle fundamentals

In the following astroparticle fundamentals, necessary to understand parts of neutrino production and interaction processes are explained in order to give an inside to the physics used for this framework.

2.1.1. Primary cosmic rays

Cosmic rays are charged particles with extraterrestrial origin. A distinction is made between stable primary particles reaching our atmosphere, and secondary particles created by interactions of the primary particles with nuclei of the atmosphere. Primary particles consist of around 79 % protons, whereas 70 % of the remaining nuclei are helium. It is believed that the majority of those particles are accelerated by diffuse shocks due to Fermi acceleration. This model leads to a particle flux Φ of $\mathrm{d}N$ particles per $\mathrm{d}E$ energy range, following a power law with the spectral index γ:

$$\Phi = \frac{\mathrm{d}N}{\mathrm{d}E} \propto E^{-\gamma}\,. \tag{2.1}$$

As seen in graphic 2.1 the measured all-particle air shower spectrum reflects the assumption of a power law, that, multiplied with $E^{2.6}$, shows steepening points called *knee* and *ankle* resulting in different spectral-indices [WBM98; Ber+12]:

$$\gamma \approx \begin{cases} 2.67, & 10^{10}\,\mathrm{eV} < E < 5 \cdot 10^{15}\,\mathrm{eV} \\ 3.10, & 5 \cdot 10^{15}\,\mathrm{eV} < E < 3 \cdot 10^{18}\,\mathrm{eV} \\ 2.67, & 3 \cdot 10^{18}\,\mathrm{eV} < E < 10^{21}\,\mathrm{eV}\,. \end{cases} \tag{2.2}$$

Upper energy limits of cosmic particles depend on their origin and interactions during

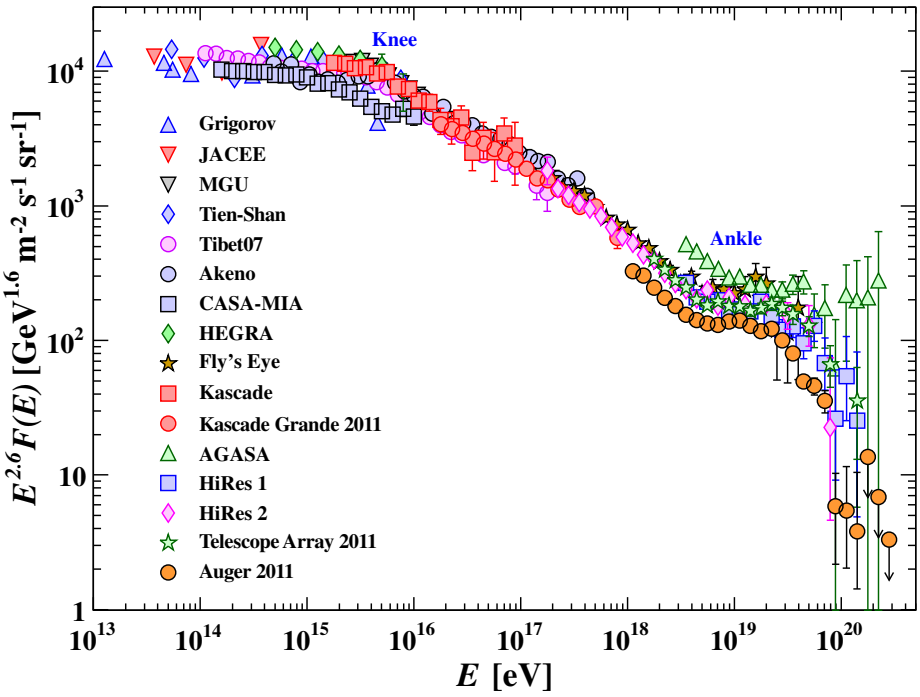

Figure 2.1.: Energy dependent spectrum of all-particles from atmospheric showers as measured by various experiments [Ber+12].

their journey to earth. The first mayor change in the spectrum, the *knee*, might be caused by an acceleration maximum of galactic accelerators. Supernova remnants for example seem to have an upper acceleration limit of 10^{15} eV for protons.

$$\mathrm{p} + \gamma_{\mathrm{CMB}} \rightarrow \begin{cases} \Delta^{+} \\ \mathrm{p} + \mathrm{e}^{-} + \mathrm{e}^{+} \end{cases} \tag{2.3}$$

Potential reasons for the *ankle* are proton interactions with photons of the 2.7 K cosmic microwave background (CMB), as shown in equation (2.3), or domination of an extragalactic flux over the galactic one [Ber+12].

2.1.2. Atmospheric neutrinos

Since cosmic rays are mainly composed of protons, it is reasonable to consider proton-nuclei interactions:

$$\mathrm{p} + N \rightarrow \begin{cases} \pi^{\pm} + X \\ \mathrm{K}^{\pm} + X \\ \mathrm{D}^{\pm} + X \end{cases} \tag{2.4}$$

where N is a nuclei of the atmosphere and X an interaction product of the inelastic scattering process. Those mesons decay and produce neutrinos amongst others. Neutrinos from charmed particles, as shown in equation (2.6), are called prompt neutrinos, whereas neutrinos from muon decays, as in (2.7), are called conventional neutrinos [BMW12].

$$\pi^{\pm}(\mathrm{K}^{\pm}) \rightarrow \mu^{\pm} + \nu_{\mu}(\overline{\nu}_{\mu}) \tag{2.5}$$
$$\mathrm{D}^{\pm} \rightarrow \mu^{\pm} + \nu_{\mu}(\overline{\nu}_{\mu}) + \mathrm{K}^{\pm} \tag{2.6}$$
$$\mu^{\pm} \rightarrow \mathrm{e}^{\pm} + \nu_{\mathrm{e}}(\overline{\nu}_{\mathrm{e}}) + \overline{\nu}_{\mu}(\nu_{\mu}) \tag{2.7}$$

As stated in [LM00] the flux of conventional neutrinos is about one spectral index steeper than the flux of cosmic rays. While prompt neutrino flux should be roughly the same, since the charmed neutrino production is direct the decay is the dominant process. It is noteworthy, that atmospheric neutrinos are part of the background for experiments observing extragalactic neutrinos due to their continuous production around the globe, whereas the main part is up to the muons produced in the cosmic air showers.

2.1.3. Extragalactic neutrinos

Assumed sources of cosmic rays and neutrinos are Active Galactic Nuclei and Gamma Ray Bursts. Several measurements prompt that those sources contain matter and radiation fields with varying densities, both of which are suitable targets for cosmic rays [LM00]. As mentioned previously, neutrinos derive from cosmic ray nuclei interactions, whilst additional options for charged pion productions, resulting in neutrino production (2.5), are [Joh11]:

$$\mathrm{p} + \gamma \rightarrow \Delta^{+} \rightarrow \mathrm{n} + \pi^{+} \tag{2.8}$$
$$\mathrm{n} + \gamma \rightarrow \Delta^{0} \rightarrow \mathrm{p} + \pi^{-} \tag{2.9}$$
$$\mathrm{p} + \mathrm{p} \rightarrow \mathrm{p} + \mathrm{n} + \pi^{+} \tag{2.10}$$
$$\mathrm{p} + \mathrm{n} \rightarrow \mathrm{p} + \mathrm{p} + \pi^{-}. \tag{2.11}$$

Following the model of Becker, Biermann and Rhode [BBR05] the diffuse neutrino flux from radio galaxies can be assumed as $\propto {E_{\nu}}^{-2}$.

Neutrinos from Active Galactic Nuclei

It is assumed that Active Galactic Nuclei (AGN) are the most powerful sources for high-energetic neutrinos, as their bolometric non-thermal energy release surmounts all other known sources. They are probably comprised of an accretion disk surrounding an *active* supermassive blackhole ($M = 10^8\,M$) radiating photons in optical frequencies. Approximately 1% of all conspicuous bright galaxies are AGN. Gravitational energy discharge due to accretion of a super massive blackhole is presumably the root of this power. A combination of magnetic fields and a shocked accretion flow might produce shock accelerated protons, that potentially interact with the thermal radiation field of the AGN or matter of the accretion disk [LM00].

Neutrinos from Gamma Ray Bursts

Gamma Ray Bursts (GRBs) are the most luminous devastating phenomena for now. A simple approach for describing GRBs is the one of a relativistic fireball which accelerates electrons, emitting synchrotron radiation. Further causes under consideration are for instance hypernovae or mergers of neutron stars. Neutrino production, as suggested by Waxman and Bahcall [WB97], is due to accelerated protons interacting with the photons from the emitted synchrotron photons [LM00].

2.1.4. Neutrino interactions

The properties, that single out neutrinos as information carriers about their origin prohibits them from being directly measured. Accordingly indirect measurements of photons emitted by Cherenkov radiation of the charged interaction products are performed. Concerning high-energetic neutrinos up until $\sim 100\,\mathrm{PeV}$, the interaction of interest is the deep inelastic scattering on nuclei. Since neutrinos are uncharged particles, they are just able to exchange W bosons, through charged-current (CC), or Z bosons, via neutral-current (NC) interactions [Joh11].

$$\nu_\ell(\overline{\nu}_\ell) + N \to \ell^-(\ell^+) + X \qquad \text{(CC)} \tag{2.12}$$

$$\nu_\ell(\overline{\nu}_\ell) + N \to \nu_\ell(\overline{\nu}_\ell) + X \qquad \text{(NC)} \tag{2.13}$$

Equations (2.12) and (2.13) display those interaction processes whereas N is a nucleon, ℓ stands for the lepton flavor and X is the hadronic interaction product.

2.2. Computational fundamentals

As shown before the index of an energy spectrum is dependent on the particles origin and interactions. Since neutrinos reaching the earth are believed not to have interacted

before they still provide information about their origin thus an analysis of them seems promising. In order to obtain the index of a neutrino flux, it needs to be measured first, then separated from the atmospheric neutrino background and later cleared up from the detectors influence, this last process in called *unfolding*. The relation between the measured neutrino flux $g(y)$ and the real flux $f(x)$ is called a *folding* and is given by a Fredholm integral equation [Fre03]:

$$g(y) = \int_c^d A(y,x) f(x)\,\mathrm{d}x + b(y)\,. \tag{2.14}$$

The variable $b(y)$ contains the background information whereas $A(y,x)$, called *response function*, describes the detector influence. The response of the detector is crucial but can't be obtained without the usage of Monte-Carlo simulations. These simulations can provide knowledge of the particle detector interactions while also being used for separation analysis.

2.2.1. Monte-Carlo simulations

Complicated or analytically unsolvable statistical problems are often treated numerically with so called Monte-Carlo simulations. The principle is to calculate a number of incidents by generating random numbers, that follow a probability density thus simulating attributes of interest [BL98]. These attributes for example can be used for calculations of detector particle interaction processes.

Random number generator

Random numbers necessary for Monte-Carlo simulations need to be uncorrelated and reproducible. Limitations for methods creating such random numbers are dictated due to various factors such as processor word length or the deterministic nature of a computer. In general a starting number, called *seed*, is chosen as a base for an iteration method. Those methods are characterised by their repeat cycle, called *period*, and their lack of correlation between consecutive numbers. The range of the created numbers is usually between 0 and 1 while the distribution is either uniform or normal [BL98].

Distributed random numbers

In order to project uniform numbers $U(0,1)$, produced by a random number generator to a given continuous probability density $f(x)$ a transformation of the following form is necessary:

$$x = F^{(-1)}(u)\,, \tag{2.15}$$

using the given identities:

$$f(x)\,\mathrm{d}x = U(0,1)\,\mathrm{d}u \quad \text{and} \quad \int_{-\infty}^{x} f(t)\,\mathrm{d}t = F(x) = u\,. \tag{2.16}$$

Since an inversion $F^{(-1)}$ of the probability density function $f(x)$ is used, this method just appeals for invertible functions. But others can be transformed with algorithms like Von Neumann's rejection technique or the polar method. A comprehensive consideration is given by Blobel and Lohrmann [BL98].

3. Simulation

The Monte-Carlo framework created within the scope of this thesis breaks down the particle measurement process into four main parts: detector construction, particle production and propagation, measurement and data preparation. This division utilizes the advantages of an object orientated programming approach by imitating involved objects of the real measurement process, thus minimizing possible misreconstructions. The structures behind the module implementations are described below.

Bearing in mind, that the framework is a continuous work in progress, whereby the particle production process is currently not part of the actual framework but already implemented in two programs called *EMSA* and *iceplay*. These programs are first applications of the framework. Their code can be found online `https://github.com/WortPixel/bachelor_thesis`. *EMSA* provides raw data (as described in 3.3) as well as prepared data (as in 3.4) with particles only produced on one side of the detector. However, *iceplay* merely provides preparated data with particles being produced on a sphere around the detector.

3.1. Detector construction

One of the main goals of cosmic particle experiments is to gain information about galactic particle sources by analysing cosmic energy spectra and particle trajectories. While an energy spectrum contains information about the particles origination process, its trajectory hints its spatial origin. Hence a detector should measure particle induced intensities at several positions to enable a track reconstruction. This leads to a detector set-up containing various spatial distributed sensors, which are able to measure time-resolved intensities of particles.

In this framework a detector is represented by an object with a three-dimensional-spacial expansion, containing intensity measuring sensors. It is possible to create a cubical-shaped detector with equally distributed sensors or, as recommended, a user shaped detector with custom placed and configured sensors. The first approach is suited for situations in which the real detector is cubical-shaped or the geometric arrangement has only small impact on the measurement. Whereas the second, more customisable approach, enables users to set up a replica of a real detector by providing actual sensor

settings via a configuration file. A sensor inherits the properties *group id* and *permeability* apart from its position. Beyond that, it is able to store both the events arrival time and the measured intensity. The measurement process is further described in section 3.3.
The feature *group id* can be used to assign several sensors to a group, for example imitating a consecutive detector part, sharing similar sensor properties. The permeability is meant to reproduce percentage energy reduction due to material impact of the sensor or its surrounding. Other useful features might be a random triggering rate simulating natural noise or a distance dependent detection efficiency.

3.2. Particle production and propagation

As stated before, the particle production is currently not part of the framework, but already implemented in *EMSA* and *iceplay*. This choice is made based on the idea, that especially the spacial origin of particles might vary a lot between experiments, hence it should be implemented into a users application. But including frequently used production scenarios into the framework is on the cards. Nevertheless particles are handled as independent objects containing their properties and being able to calculate their energy loss due to propagation. At the moment a particle is defined by its starting energy, position and direction. The considered energy range starts at 10 GeV.

Production

The production process, as implemented in *EMSA* and *iceplay*, is based on distributed random numbers. *Mersenne Twister*, as provided by Boosts[1] `mt19937`[2] and ROOTs[3] `TRandom3`[4], is the random number generator of choice. Both implementations are based on the paper [Mau00].
The direction of a particle is specified by its azimuthal and polar angle. Both *EMSA* and *iceplay* generate normal distributed random numbers as starting values for the directional angles, imitating a Gaussian smeared point source. Starting points of particles are normal distributed as well, at least for *EMSA*, *iceplay* uses the same distribution technique, but for the generation of a temporary starting point on a sphere. Due to this, the actual starting point needs to be calculated as the cross-section between the temporary starting point on the sphere and the nearest detector surface.

[1] Boost is a peer-reviewed collection of `C++` libraries. Its trustworthiness is hinted by the fact, that some of its libraries already found their way into the official `C++` standard, more on that `http://www.open-std.org/jtc1/sc22/wg21/`. For example the library `random`, providing the random number generator used for the framework of this thesis, is now part of the `C++11` standard.

[2] `mt19937`s header file can be found on `http://www.boost.org/doc/libs/1_54_0/boost/random/mersenne_twister.hpp`

[3] ROOT [BR96] is a framework for high-energy nuclei and particle processing and analysis, developed at the Conseil Européen pour la Recherche Nucléaire (CERN).

[4] `TRandom3`s documentation can be found on `http://root.cern.ch/root/html/TRandom3.html`

However, energy values of particles should follow a power law, as explained in 2.1.2 and 2.1.3. The function $x(r)$, mapping random uniform numbers r to a power law distribution $A(x)$, can be derived using the formalism explained in 2.2.1, whereas a normalisation factor A is introduced, enabling the choice of a range.

$$A(x) = \Phi_0 \int_a^x E^{-\gamma}\,\mathrm{d}E = \frac{\Phi_0}{1-\gamma}\left(\frac{1}{x^{1-\gamma}} - \frac{1}{a^{1-\gamma}}\right) \tag{3.1}$$

$$A = A(b) = \frac{\Phi_0}{1-\gamma}\left(\frac{1}{b^{1-\gamma}} - \frac{1}{a^{1-\gamma}}\right) \tag{3.2}$$

$$r = \frac{A(x)}{A} = \frac{x^{1-\gamma} - a^{1-\gamma}}{b^{1-\gamma} - a^{1-\gamma}} \tag{3.3}$$

$$\Rightarrow x(r) = \left[\left(b^{1-\gamma} - a^{1-\gamma}\right)\cdot r + a^{1-\gamma}\right]^{\frac{1}{1-\gamma}} \tag{3.4}$$

The range of the energy spectrum can then be set by providing the variables a for the lower limit and b for the upper limit through the configuration file.

Propagation

After a muon, from cosmic radiation or neutrino interaction, enters the detector, it loses energy due to various interaction processes like ionization, photonuclear interaction, pair-production and other processes. For an in-depth look consult [CR04]. Amongst other things it provides the following linear equation describing a general approximation of muon energy loss for energies above $\sim 10\,\mathrm{GeV}$:

$$-\frac{\mathrm{d}E}{\mathrm{d}x} = a + b\cdot E\,. \tag{3.5}$$

Where $a = 0.259\,\mathrm{GeV/mwe}$ and $b = 0.363\cdot 10^{-3}\,/\mathrm{mwe}$. While the value for a is also confirmed by Koehne et al. [Koe+13], the value for b is slightly increased $b = 0.364\cdot 10^{-3}\,/\mathrm{mwe}$.
Particles produced by the framework follow this propagation model, owing to its suitability for the considered energy range, while using the more current values.

3.3. Measurement

Single particles interacting with the detector are called *events*, while several particles interacting almost simultaneously are called *coincidental events*. The framework provides both event-wise and coincidental measuring methods. After a measuring process each activated sensor contains a calculated intensity as well as an arrival time. Whereas the measured intensity is the energy of a photon emitted by a particle passing a sensor at the nearest position possible. Here, a model using a reduction of the actual Cherenkov radiation, caused by the propagation of relativistic charged particles, to a perpendicular energy radiation is chosen to minimize the frameworks complexity. Whether a sensor triggers or not is based on an energy dependent acceptance, more on that below.

3.3.1. Arrival time

It is reasonable to assume, that particles within the considered energy range of above 10 GeV, as for the IceCube detector, propagating through ice are travelling almost with the speed of light. Due to this, the arrival time is calculated by the track length, starting at the detector entrance point and ending at the nearest position between the track and the addressed sensor, and the distance from this perpendicular point to the sensor position itself.

3.3.2. Intensity

As stated before the measuring process is dependent on an energy based triggering process. Therefore the energy of interest E of a particle at the dropped perpendicular point $x_\perp$ between a sensor and the particles track is used to generate a measuring probability [Rho12]:

$$P\left(E(x_\perp)\right) = \left(1 - \exp\left(-\frac{E(x_\perp)}{2}\right)\right)^3 . \tag{3.6}$$

Afterwards this probability is compared with a uniform random number. If the probability exceeds the random number, the actual measurement takes place. For this, the following equation is used:

$$I(E(x_\perp)) = \frac{p(\mathrm{s}) \cdot E(x_\perp)}{1 + d(x_\perp, x_\mathrm{s})^2} . \tag{3.7}$$

This equation is heuristically build up, considering the typical distance dependent energy loss for intensities and likely boundary values. In this case the distance to the source of radiation is given by the distance d between the dropped perpendicular point $x_\perp$ where the particle emits a Cherenkov photon and the sensor position x_s. Using just the typical distance dependency does not work in this case, since a direct particle-sensor hit would cause the measurement of an infinite energy. To circumvent this the denominator is increased by one, resulting in a match to the obvious boundary condition:

$$I(E(x_\perp = x_\mathrm{s})) \stackrel{!}{=} E(x_\perp) . \tag{3.8}$$

Other boundaries are dictated by the material influence emulated through the permeability factor p for a given sensor s. As this parameter should enable a percentage energy reduction resulting in a range of 0 to 1 it can just be multiplied to the measured energy $E(x_\perp)$. Whereas the lower border 0 stands for a complete energy absorption while the upper limit 1 mimics a total energy permeability. The arrival times and intensities stored in all the sensors are from now on referred to as *raw data*.

After a measurement, raw data can be read out and processed into attributes with various meanings. Before another measurement takes place the sensors need to be reset except a coincidental event should be measured.

3.4. Data preparation

Raw data, as described above, can be computed into more meaningful attributes for analysis. In the following, attributes, processed both within the framework and its applications *EMSA* and *iceplay*, are described. This separation is due to the fact, that the particle production is currently not handled by the framework itself, more on that in section 3.2 above.

Beginning with attributes calculated by *EMSA* and *iceplay*, there are, listed by their names used for data exportation: *N_Sensors*, *N_Groups*, *N_Sensors_per_Group*, *Q_total*, *1stSensor* and *Effective_Track_Length*. Due to its dependencies, the last-named attribute is explained after the description of the framework-provided attributes. Attributes starting with an *N* contain amounts, for *N_Sensors* of activated sensor, for *N_Groups* of groups with at least one activated sensor, while *N_Sensors_per_Group* lists the amounts of activated sensors per group. *Q_total* stores the cumulative intensity a track deposited in the whole detector whilst *1stSensor* emerges three times, one time for each coordinate of the first activated sensor.

Framework provided attributes are: *CoI* along with *R_AzimuthalAngle* and *R_PolarAngle*. Whereby *CoI* stands for *Center of Intensity* and can be seen as a center of mass weighted with intensities instead of masses. In order to explain the remaining values it is necessary to introduce the applied first guess track reconstruction.

3.4.1. Particle track reconstruction

As explained above a track reconstruction is worthwhile since it reveals hidden spatial information about a particles origin. Currently the particles track is reconstructed through projections of the three-dimensional track onto two two-dimensional planes. These planes are the xy- and the yz-planes of the used coordinate system, they are separately analysed using the well known analytic solution for linear regressions. The obtained linear functions define the dependencies $y(x)$ and $z(y)$ for the tracks. Thus it is enough to choose an arbitrary identity for one coordinate to obtain a position located on the track. Since a track not only consists of a suspension point, a direction is needed, too. The deviations of the linear functions are chosen as azimuthal and polar angles providing the necessary direction and the attributes *R_azimuthalAngle* and *R_polarAngle* at the same time. The *R* stands for *reconstructed*. Utilizing the reconstruction the previously mentioned effective track lengths can now be approximated. Therefore the distance between the projections of the first and last activated sensors onto the reconstructed track is given as the *Effective_Track_Length*.

3.5. A first comparison with real data

In the following a z-distribution of the center of intensity produced with *iceplay* is compared with the distribution of an actual burnsample of IceCube. A burnsample is a fraction of an actual measurement data set which is used for analysis. This comparison serves as a first hint of conformity. For further analysis a future in depth review of the created Monte-Carlo data is necessary. The data set of interest created with *iceplay* imitates a signal deriving from an angle range of π. Distribution plots of all created features are located in the appendix. The detector set up consists of 100 groups representing strings each containing 60 sensors. Horizontal distances between sensors are 100 m while the vertical distances are 10 m. Dust layers with permeabilities of 0.2 affect all sensors at the same height. They are placed at heights of 430 m, 490 m and 540 m while a consecutive dust layer is placed between 250 and 350 m.

At first glance some similarities between both distributions displayed in 3.1 and 3.2 are visible. The influence of the consecutive dust layer as seen in the burnsample in figure 3.1, between the z-positions -200 m and 0 m can be found in figure 3.2 in the range of $z \in [120\,\text{m}, 440\,\text{m}]$. Whereas the area of the consecutive dust layer seems to be connected with the layer at 430 m resulting in a wider steepening of the distribution. In the region above 440 m the peaks match the area between 100 and 350 m of the burnsample distribution for the most part. In order to highlight the similarities a trimmed distribution of the burnsample is shown in figure 3.3. Mayor differences occur at the edges of the distributions especially on the right side. One explanation might be linked to the fact, that the right side of the distribution translates into the upper region of the IceCube detector. This region is located around 1450 m beneath the surface of the earth. Whereas muons with an energy of 1 TeV for example are able to travel an average of 2.4 km in ice [Joh11]. Though those atmospheric muons could influence the upper region of the detector.

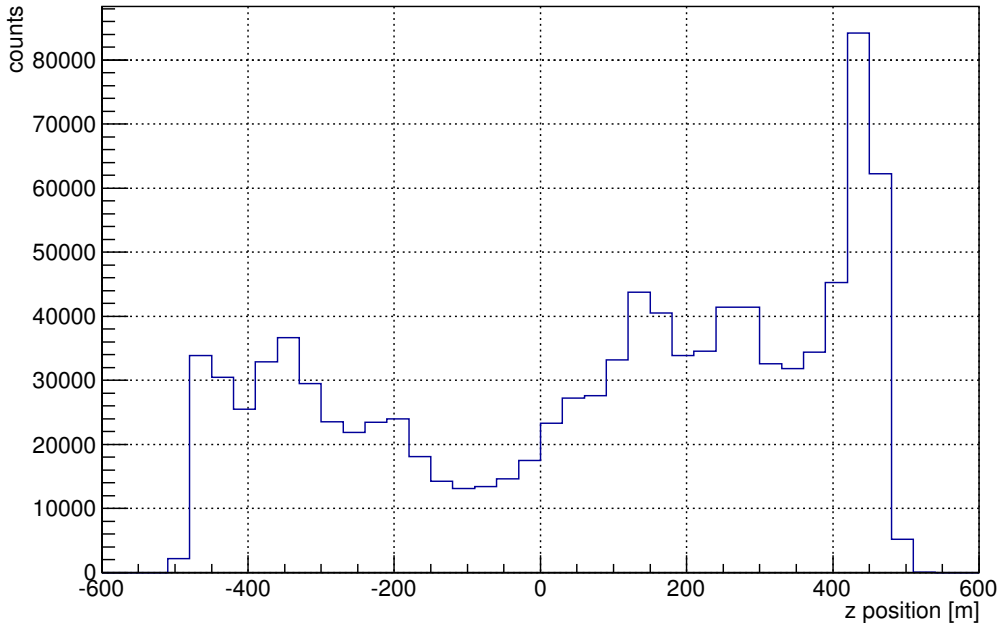

Figure 3.1.: Center of intensity z-distribution of an IceCube burnsample.

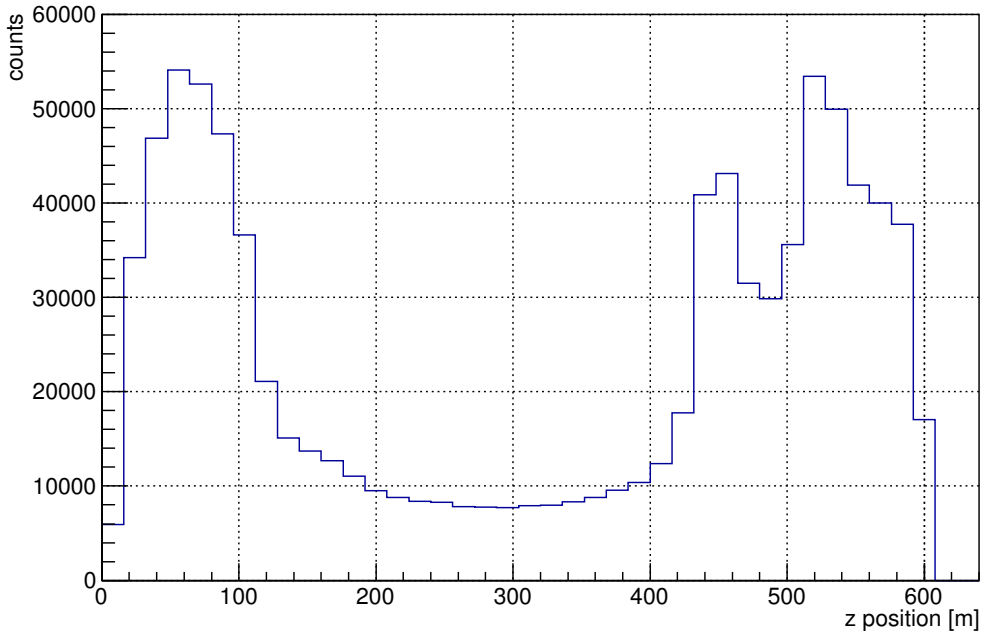

Figure 3.2.: Center of intensity z-distribution produced with *iceplay*.

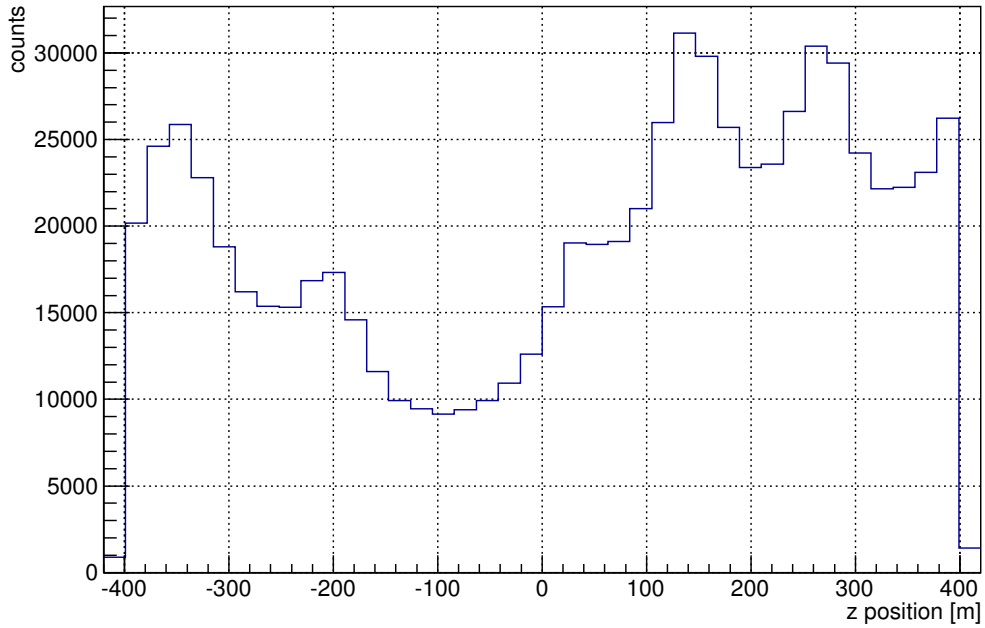

Figure 3.3.: Center of intensity z-distribution of an IceCube burnsample with a cut off before $-420\,\mathrm{m}$ and after $420\,\mathrm{m}$.

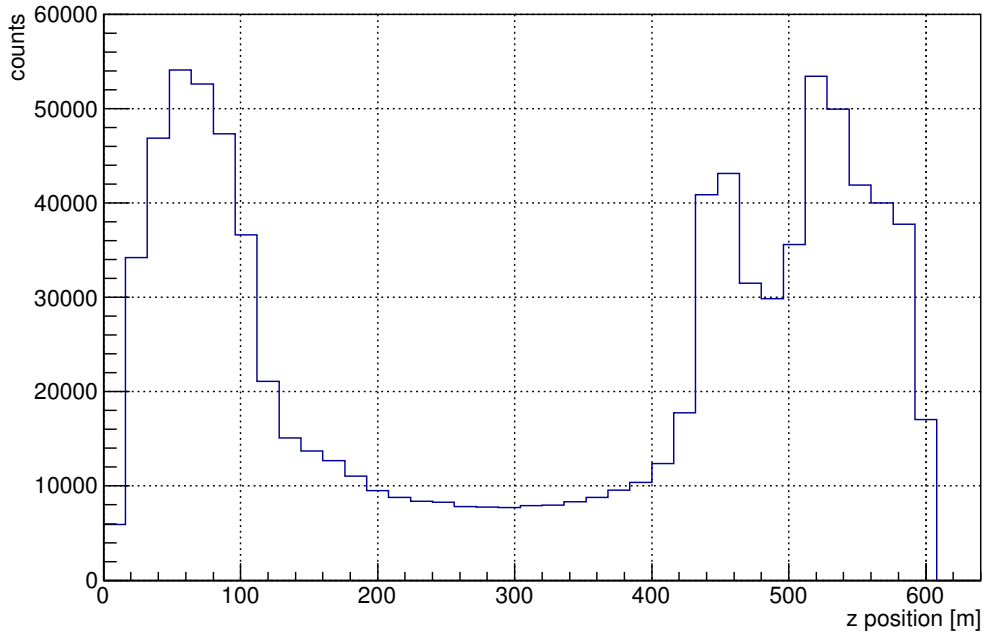

Figure 3.4.: Center of intensity z-distribution produced with *iceplay*.

4. Conclusion and outlook

Conclusion

The goal for this thesis was to create a Monte-Carlo simulation framework for particle-detector-interactions, which enables users to produce data for testing and developing analysis methods. At the same time the framework should be easy to adopt and understand, though enabling its use for tutorial purposes.

Within the scope of this thesis a Monte-Carlo simulation framework has been created. It offers objects and methods to imitate a particle-detector-interaction by providing a detector containing sensors as well as particles. Possible detector configurations are a cubical-shaped detector with equally distributed sensors and a customisable detector with user adjustable sensors. The sensors are able to measure intensities of particles propagating through the detector, while taking influences of the environment via percentage energy reduction into account. Single events as well as coincidental events can be sensed during each measurement process. After such a process all triggered sensors contain a distance, energy and environment dependent intensity. The collected data is processed into attributes for future analysis. Created particles propagate along a linear trajectory while experiencing linear energy loss. The particle production is currently outsourced into the programs *EMSA* and *iceplay* which are build around the framework as part of this thesis. To include the production process into the framework information about the geometry of natural production processes need to be considered.

Attributes generated from the simulated data are calculated allowing first analysis. Evaluating the z-distribution of the center of intensity Monte-Carlo data produced with *iceplay* shows first similarities to an IceCube burnsample.

Regarding simplicity and ease of use the framework turned out to be convenient while building up the mentioned programs. Especially during the process of creating *iceplay* only minor changes to *EMSA* were necessary for setting up a much more custom detector with various dust layers of different permeabilities. Furthermore the framework is created with expandability in mind. Methods included allow easy data transfer between individual modules while being as general as possible within the borders of the given physics. Using the framework for different purposes should be easy, since it is open source and all classes, attributes and methods are well documented.

Outlook

Since the framework developed within the scope of this thesis is built using an object orientated approach while keeping extensibility in mind, it is quite simple to both extend its abilities and even to reshape it for specialised needs. Possible extension scenarios include downloading the code and manipulating it right there or using the framework as is overloading its methods or utilizing a software design pattern called *decorator*. In virtue of the sheer diversity of possible additions a few are listed below:

- Inclusion of commonly used particle production scenarios. For example background particles deriving from an angular distribution of 4π emulating the atmospheric particles and signal particles emitted from a small region simulating a distant point source of neutrinos.
- Addition of various default detector geometries for the detector construction. For example a cylindrical structure emulating parts of the geometry of ATLAS[1].
- Introduction of structures enabling interconnections of multiple detectors. Thus using different type of sensor for different measurements or tasks like triggering.
- Enhancements to the measuring process by adding random sensor triggering simulating natural noise or implementing an actual Cherenkov cone instead of the currently used perpendicular radiation model.
- Replacing the linear particle propagation with an integral, non-linear approach.
- Improving the accuracy of material influences on the Cherenkov photons by considering the Beer-Lambert-Bouguer law, which takes logarithmic reduction due to the absorption cross section of material into account.
- Adding further attributes to the data preparation process, for example the distance between a reconstructed track and the detectors center or the center of intensity.
- Increasing the number of properties particles inherit.
- Technical improvements like decoupling the framework from libraries, for example replacing *Boost* by using the new `C++11` standard providing libraries for random number generation or allowing further output formats like the open HDF5[2] standard.

[1] `http://www.atlas.ch/detector.html`
[2] `http://www.hdfgroup.org/HDF5/`

Bibliography

[BBR05] J. K. Becker, P. L. Biermann, and W. Rhode. "The diffuse neutrino flux from FR-II radio galaxies and blazars: A source property based estimate". In: *Astropart.Phys.* 23 (2005), pp. 355–368. DOI: 10.1016/j.astropartphys.2005.02.003. eprint: arXiv:astro-ph/0502089v1.

[Ber+12] J. Beringer et al. "Cosmic Rays". In: *Phys. Rev. D* 86 (2012). URL: http://pdg.lbl.gov/2013/reviews/rpp2012-rev-cosmic-rays.pdf (visited on 07/22/2013).

[BL98] V. Blobel and E. Lohrmann. *Statistische und numerische Methoden der Datenanalyse (Teubner Studienbücher Physik) (German Edition)*. 1998th ed. Vieweg+Teubner Verlag, Sept. 1998. ISBN: 9783519032434.

[BMW12] V. Barger, D. Marfatia, and K. Whisnant. *The physics of neutrinos*. Princeton: Princeton University Press, 2012, p. 224. eprint: http://lib.myilibrary.com/detail.asp?id=385252. URL: http://www.ub.tu-dortmund.de/katalog/titel/1377761 (visited on 07/25/2013). 2012.

[BR96] R. Brun and F. Rademakers. "ROOT - An Object Oriented Data Analysis Framework". In: *AIHENP'96 Workshop, Lausanne*. Vol. 389. 1996, pp. 81–86. URL: http://root.cern.ch/. Version 5.34.07.

[CR04] D. Chirkin and W. Rhode. "Propagating leptons through matter with Muon Monte Carlo (MMC)". In: *ArXiv High Energy Physics - Phenomenology e-prints* (July 2004). Provided by the SAO/NASA Astrophysics Data System. eprint: arXiv:hep-ph/0407075. URL: http://adsabs.harvard.edu/abs/2004hep.ph....7075C.

[Fre03] I. Fredholm. "Sur une classe d´equations fonctionelles". In: *Acta Mathematica* 27 (1 1903), pp. 365–390. DOI: 10.1007/BF02421317.

[Joh11] H. Johansson. "Searching for an Ultra High-Energy Diffuse Flux of Extraterrestrial Neutrinos with IceCube 40". PhD thesis. Stockholm University, 2011.

[Koe+13] J.-H. Koehne et al. "PROPOSAL for muon propagation". In: *Computer Physics Communications* 184 (9 Sept. 2013). DOI: 10.1016/j.cpc.2013.04.001. URL: http://dx.doi.org/10.1016/j.cpc.2013.04.001.

[LM00] J. G. Learned and K. Mannheim. "High-energy neutrino astrophysics". In: *Annual Review of Nuclear and Particle Science* 50 (Dec. 2000), pp. 679–749. DOI: 10.1146/annurev.nucl.50.1.679. URL: http://dx.doi.org/10.1146/annurev.nucl.50.1.679 (visited on 07/25/2013).

[Mau00] J. Maurer. *Boost/Random - Generators*. 2000. URL: http://www.boost.org/doc/libs/1_54_0/doc/html/boost_random/reference.html#boost_random.reference.generators (visited on 08/01/2013).

[Mil12] N Milke. "Unfolding of the atmospheric neutrino flux spectrum with the new program TRUEE and IceCube". PhD thesis. Universität Dortmund, 2012. URL: http://hdl.handle.net/2003/29601 (visited on 08/09/2013).

[Rho12] W. Rhode. *Statistische Methoden der Datenanalyse*. [lecture]. The acceptance formular is from homework number 6, task number 21. Oct. 2012.

[WB97] E. Waxman and J. Bahcall. "High Energy Neutrinos from Cosmological Gamma-Ray Burst Fireballs". In: *Phys. Rev. Lett.* 78 (12 Mar. 1997), pp. 2292–2295. DOI: 10.1103/PhysRevLett.78.2292. URL: http://link.aps.org/doi/10.1103/PhysRevLett.78.2292.

[WBM98] B. Wiebel-Sooth, P. L. Biermann, and H. Meyer. "Cosmic rays. VII. Individual element spectra: prediction and data". In: *Astronomy and Astrophysics* 330 (Feb. 1998), pp. 389–398. eprint: arXiv:astro-ph/9709253. URL: http://adsabs.harvard.edu/full/1998A&A...330..389W (visited on 07/26/2013).

Eidesstattliche Versicherung

Ich versichere hiermit an Eides statt, dass ich die vorliegende Bachelorarbeit mit dem Titel „PaDIF A Particle Detector Interaction Framework for cosmic rays“ selbständig und ohne unzulässige fremde Hilfe erbracht habe. Ich habe keine anderen als die angegebenen Quellen und Hilfsmittel benutzt sowie wörtliche und sinngemäße Zitate kenntlich gemacht. Die Arbeit hat in gleicher oder ähnlicher Form noch keiner Prüfungsbehörde vorgelegen.

Ort, Datum	Unterschrift

Belehrung

Wer vorsätzlich gegen eine die Täuschung über Prüfungsleistungen betreffende Regelung einer Hochschulprüfungsordnung verstößt handelt ordnungswidrig. Die Ordnungswidrigkeit kann mit einer Geldbuße von bis zu 50 000,00 € geahndet werden. Zuständige Verwaltungsbehörde für die Verfolgung und Ahndung von Ordnungswidrigkeiten ist der Kanzler/die Kanzlerin der Technischen Universität Dortmund. Im Falle eines mehrfachen oder sonstigen schwerwiegenden Täuschungsversuches kann der Prüfling zudem exmatrikuliert werden (§ 63 Abs. 5 Hochschulgesetz - HG -).

Die Abgabe einer falschen Versicherung an Eides statt wird mit Freiheitsstrafe bis zu 3 Jahren oder mit Geldstrafe bestraft.

Die Technische Universität Dortmund wird ggf. elektronische Vergleichswerkzeuge (wie z.B. die Software „turnitin“) zur Überprüfung von Ordnungswidrigkeiten in Prüfungsverfahren nutzen.

Die oben stehende Belehrung habe ich zur Kenntnis genommen.

Ort, Datum	Unterschrift

A. Iceplay Monte-Carlo feature distributions

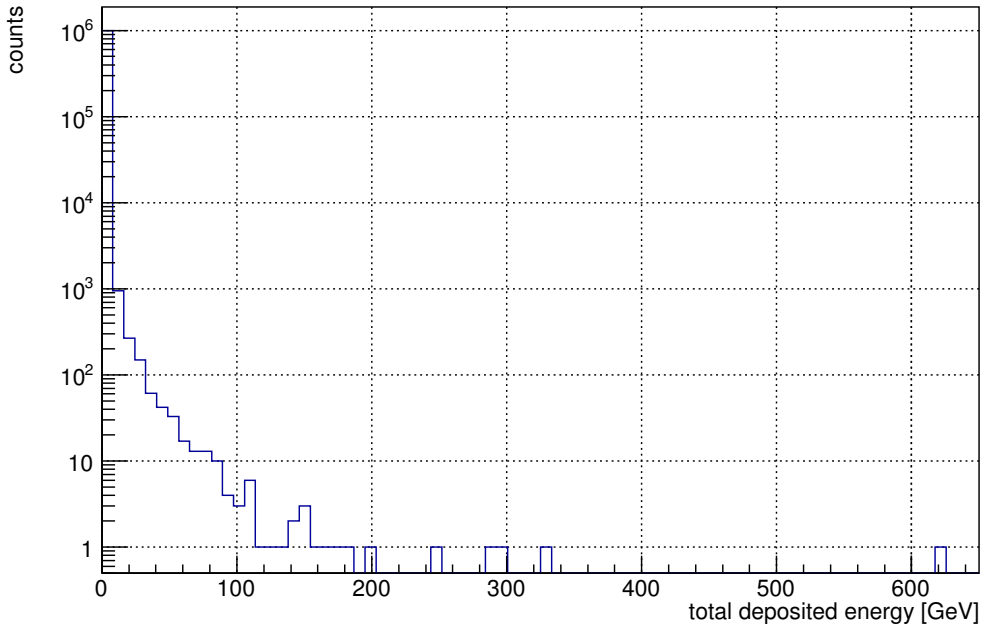

Figure A.1.: Distribution of totally measured energy per measurement.

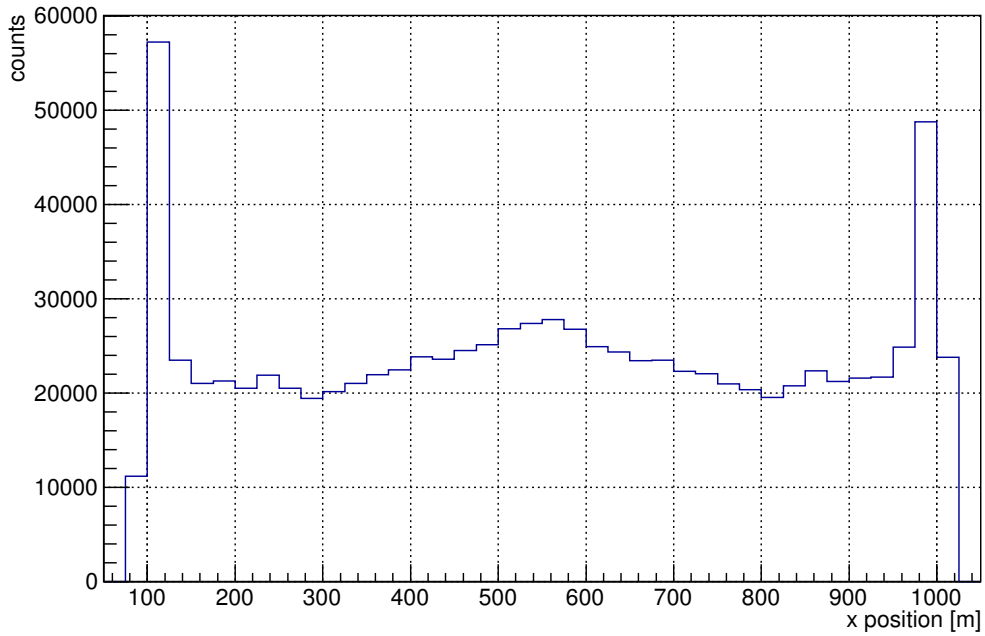

Figure A.2.: Center of intensity x-distribution produced with *iceplay*.

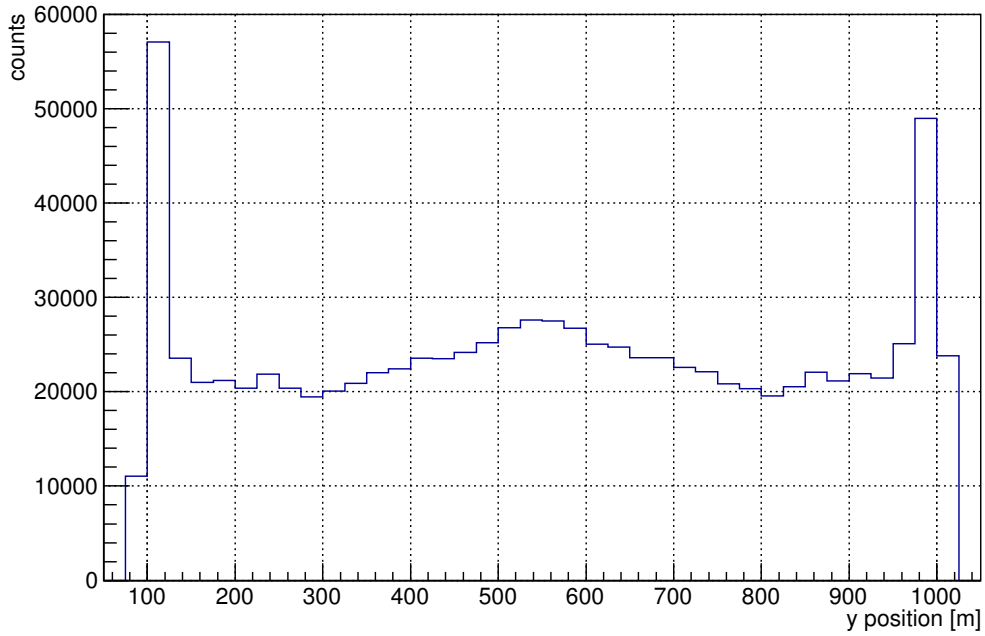

Figure A.3.: Center of intensity y-distribution produced with *iceplay*.

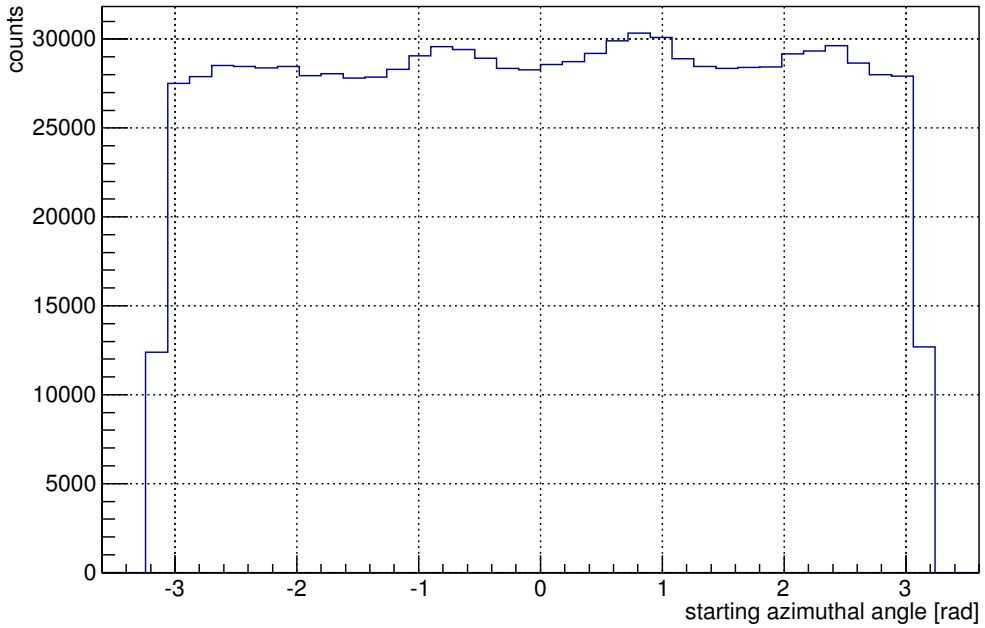

Figure A.4.: Azimuthal angle distribution of particles starting direction produced with *iceplay*.

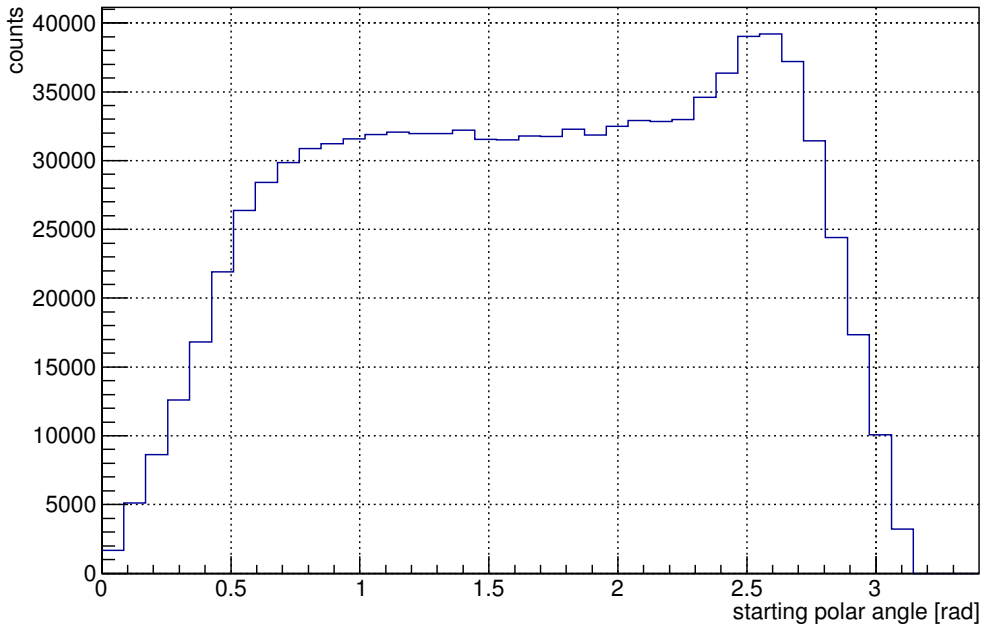

Figure A.5.: Polar angle distribution of particles starting direction produced with *iceplay*.

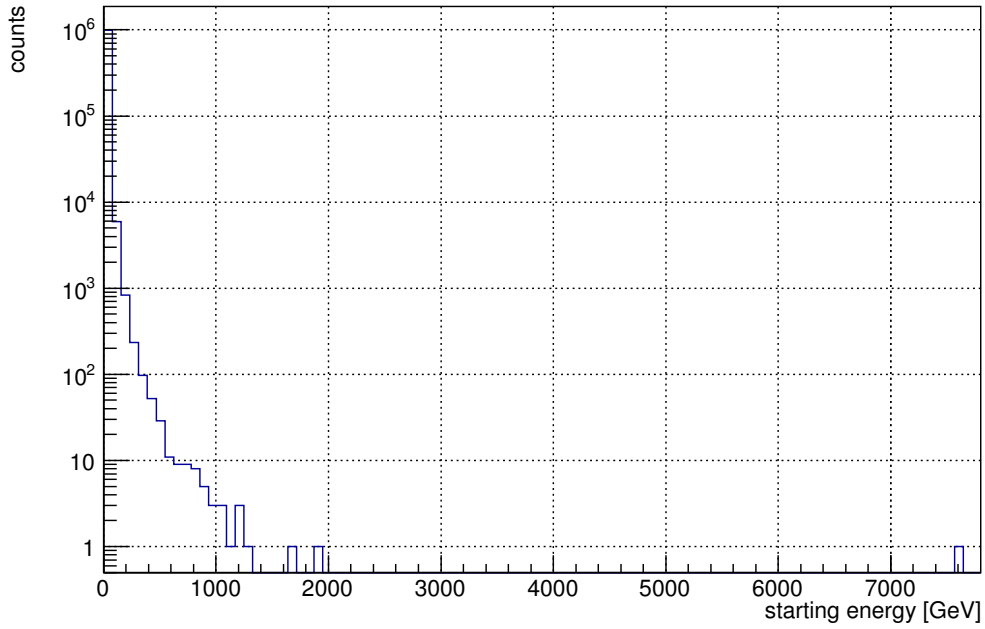

Figure A.6.: Distribution of particles starting energy produced with *iceplay*.

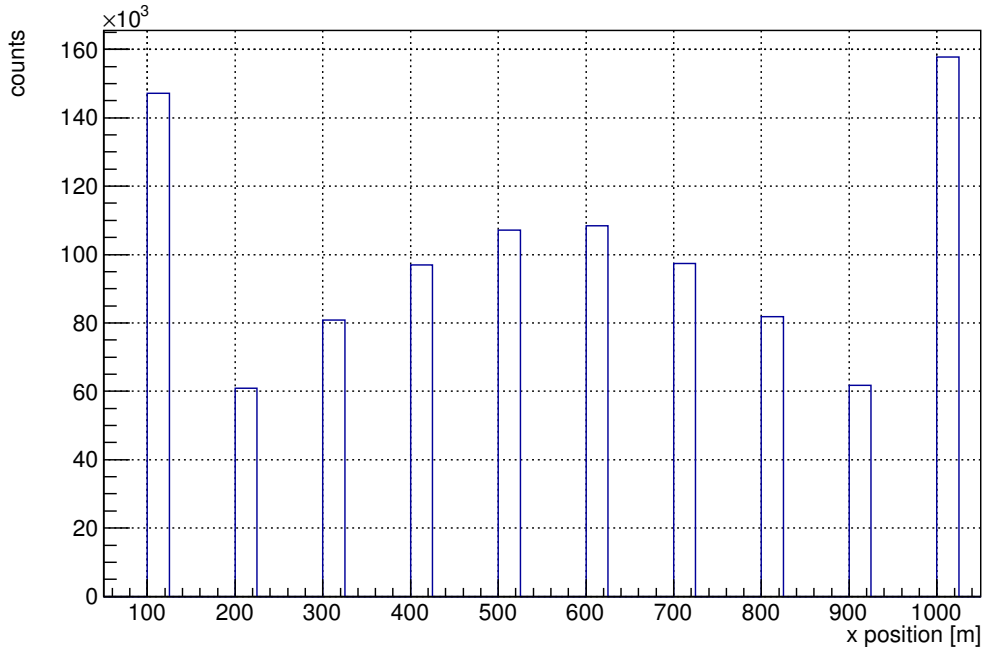

Figure A.7.: x-distribution of particles starting position produced with *iceplay*.

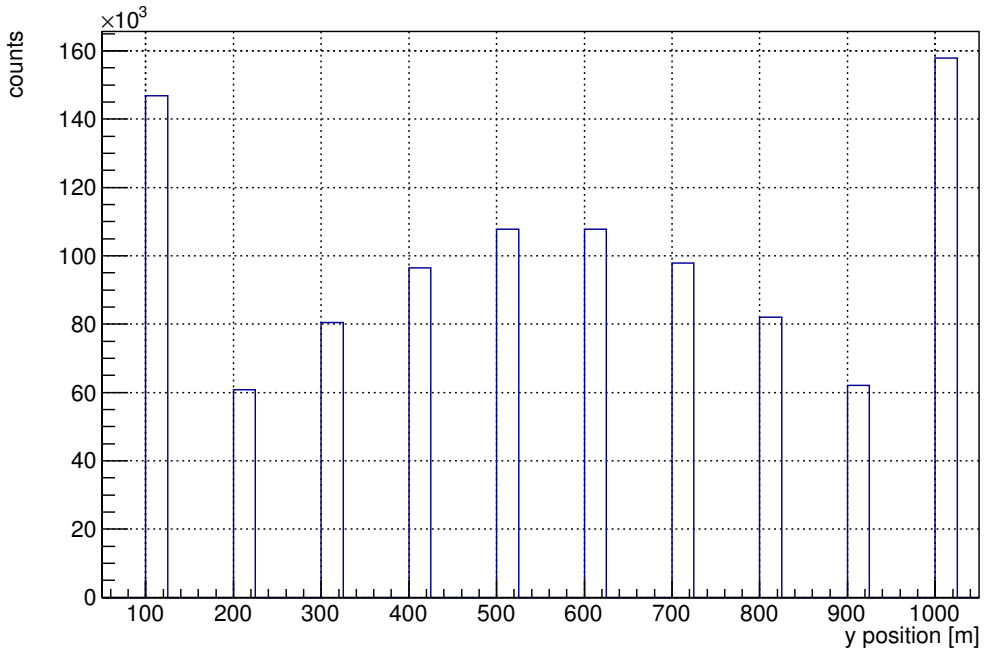

Figure A.8.: *y*-distribution of particles starting position produced with *iceplay*.

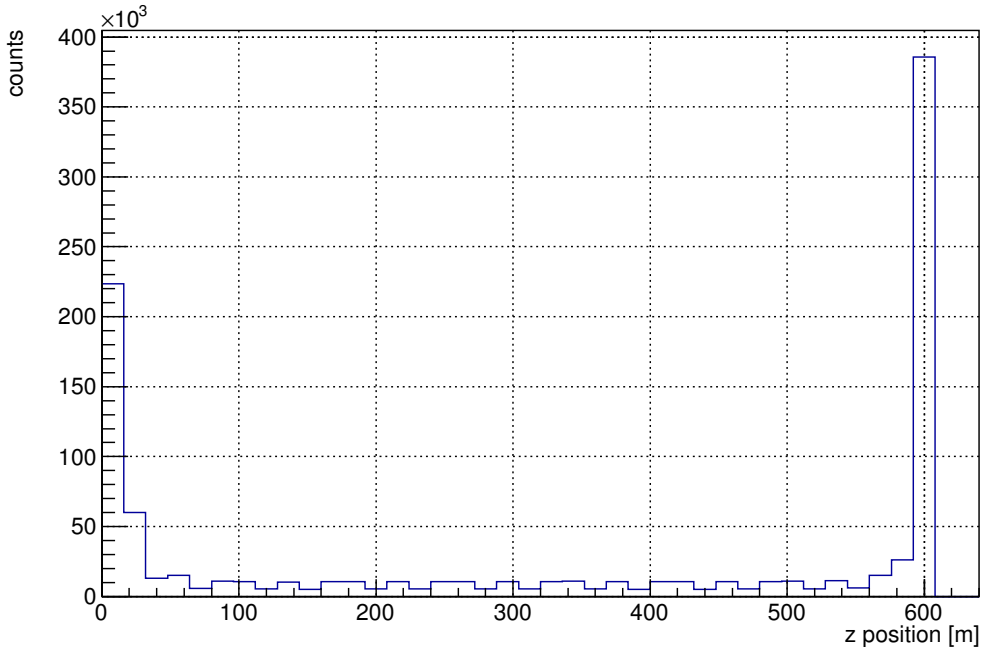

Figure A.9.: *z*-distribution of particles starting position produced with *iceplay*.

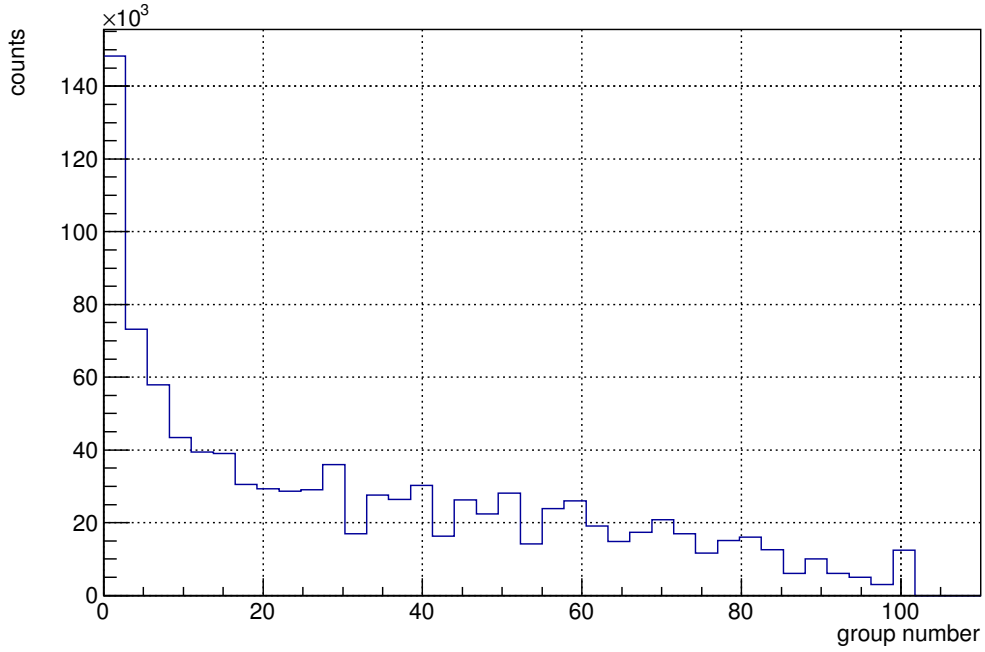

Figure A.10.: Distribution of activated groups per measurement.

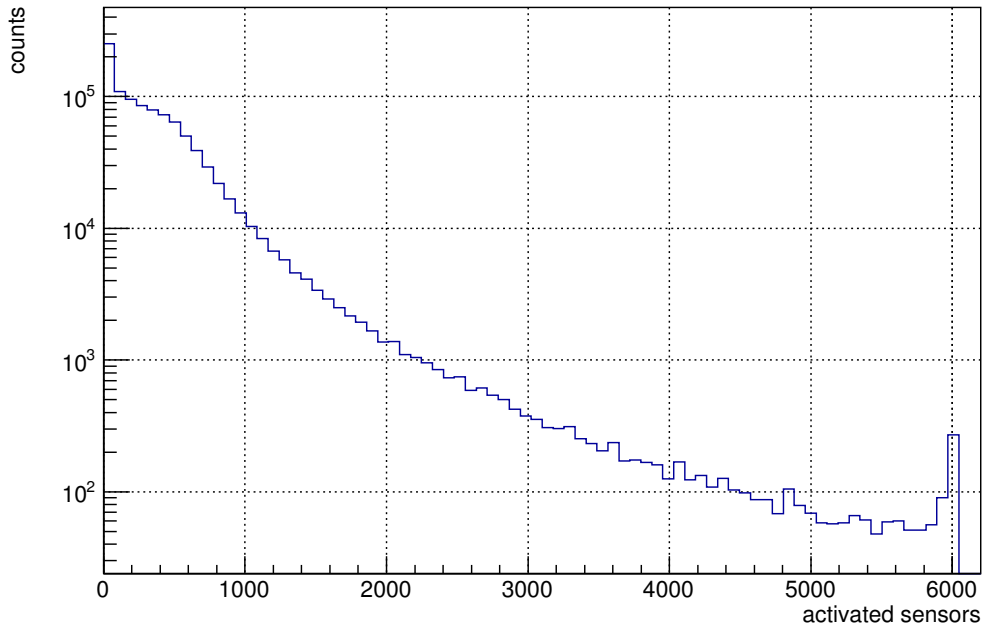

Figure A.11.: Distribution of activated sensors per measurement.

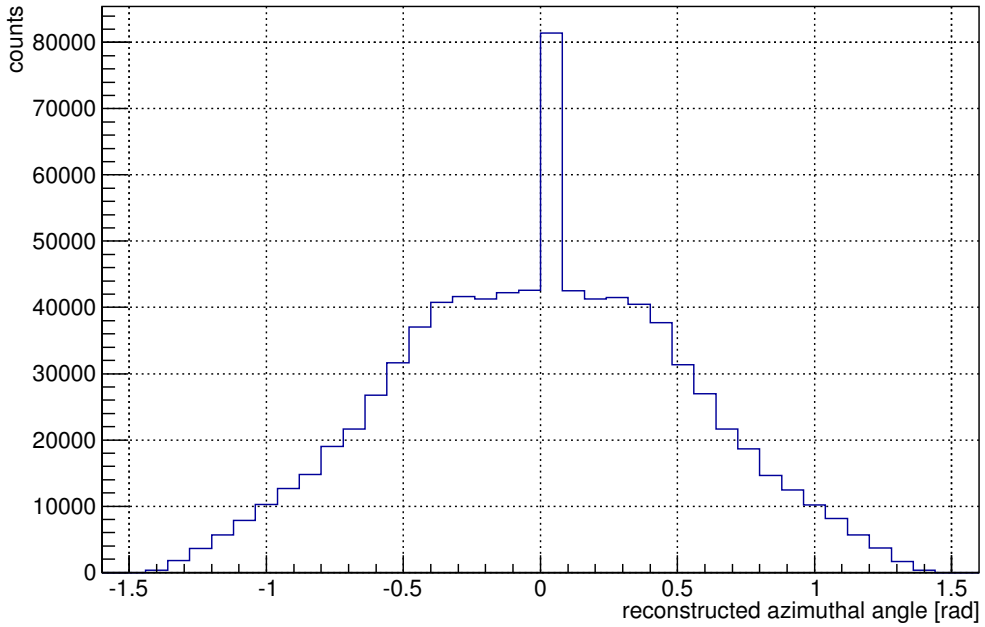

Figure A.12.: Reconstructed azimuthal angle distribution produced with *iceplay*.

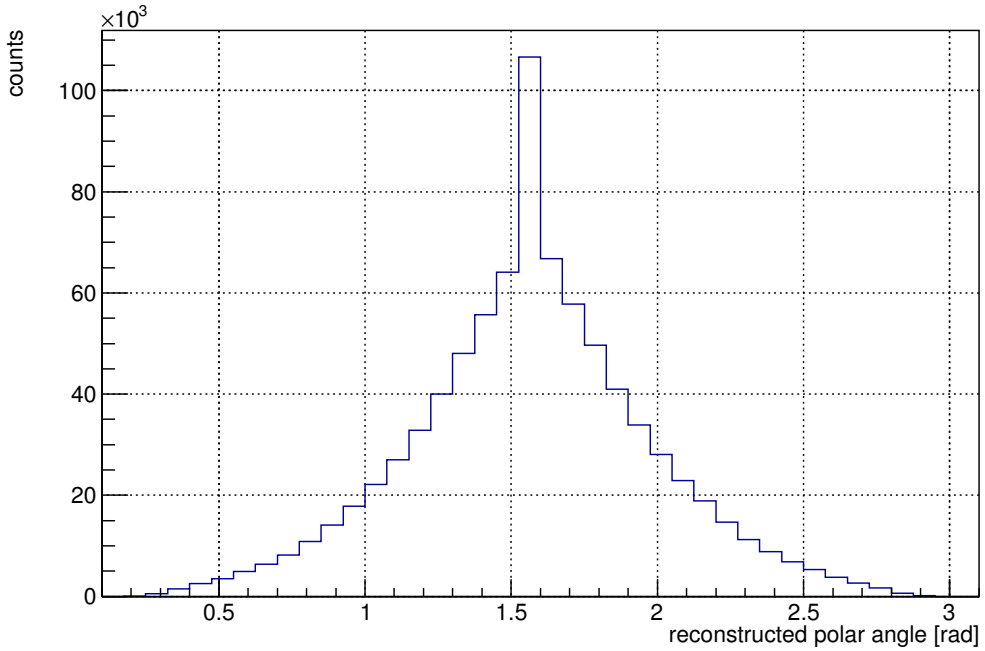

Figure A.13.: Reconstructed polar angle distribution produced with *iceplay*.